

STATIC AND DYNAMIC TESTING OF COAL SPECIMENS

Z. Zheng, M. Khodaverdian and J. D. McLennan

Terra Tek, Inc, Salt Lake City, Utah

ABSTRACT

Substantial public domain information exists, documenting discrepancies in measured values of elastic properties determined from static and dynamic measurements made on conventional reservoir rocks. There is relatively limited public domain information available for coal, especially the relationship between static and dynamic properties as stress conditions are changed. In studying coal mechanical behavior, one difficulty arises because of the extremely friable nature of coal. In searching for "optimal" sample preparation procedures, several techniques have been used. These techniques have included coring samples using nitrogen, stepwise grinding to the desired dimensions, and, water-saturated freezing and subsequent coring to avoid disintegration of the coal. The most effective procedure attempted to date is the stepwise grinding. To understand static-dynamic mechanical behavior characteristics in coal, ultrasonic wave velocities were measured on relatively "undisturbed" coal samples concurrently with triaxial and hydrostatic compression. Effects of saturation on coal static-dynamic behavior were also examined. Dynamic bulk and Young's moduli and Poisson's ratio were calculated from the wave velocities. The dynamic moduli of the tested samples were greater than the static moduli and increased with increasing effective confining stress. This increase was greatest during initial increments of effective confining stress. P-wave velocity increased with an increase in pore pressure. However, S-wave velocity decreased with an increase in pore pressure. Such a decrease in S-wave velocity resulted in an increase in dynamic Poisson's ratio as calculated from elastic relationships.

INTRODUCTION

During the past decades, concentrated efforts have been undertaken to extract methane from coal in multiple basins throughout the United States. Initial degasification concepts were to remove gas in advance of underground mining activities. This allowed more rapid removal of coal by efficient use of longwall mining methods. This evolved to extraction of the methane to supplement the gas supply from deeper unminable coal seams. This genesis required developing techniques to allow for the different behavioral characteristics of coal. As such, logging, completion and stimulation practices routinely used in more conventional reservoirs have been tailored for methane extraction from coal. This paper deals with one

aspect of this; the utilization of acoustic wave velocities for the determination of in-situ mechanical properties of coal.

STATIC AND DYNAMIC MECHANICAL PROPERTIES

It has been an acknowledged fact for more than half a century that differences exist between statically and dynamically-determined mechanical properties. Ide, 1936 reported:

“...the dynamically determined elastic modulus is in general higher than that statically determined and the two methods gave the most divergent results for those rocks which possess the lowest elasticity. Our previous discussion indicates that both conclusions are explicable in terms of enhanced yield of the more porous rock under static stress, due to the gradual closing of cracks and cavities.”

Cannaday, 1964, carried out systematic testing on Indiana limestone. Among his observations was the assertion that no correlation whatever could be made between sonically and statically determined values of Poisson's ratio. Simmons and Brace in 1965 published experimental data contrasting static and dynamic rock compressibility measurements. In the same year, King published comparative experimental data for conventional petroleum rock types (i.e. Boise and Berea sandstones), particularly emphasizing observations that for the moduli at least, discrepancies become less as the applied effective normal stress becomes larger. More recently, Lin, 1985, reported comparisons made on Mesa Verde rocks, emphasizing that the dynamic moduli were larger, and sometimes substantially so, than the static moduli. In 1989, Jeffrey and McLennan reported static and dynamic measurements made concurrently on triaxially loaded sandstones. The observations are comparable trends in E_s and E_D to those reported by others and poor development of significant relationships for Poisson's ratio.

These are only a few of the many references concerning the differences between static and dynamic mechanical properties. As can be seen or inferred from the above references, there can be a number of influential factors:

- **Experimental Procedures:** Over the years, there have been improvements in the accuracy of experimental procedures for static and dynamic testing, allowing more direct comparison of values. For example, some of the early testing contrasted dynamic elastic moduli with secant rather than tangent static moduli.

- **Wave Propagation:** Even presuming basic experimental accuracy, it must be recognized that static and dynamic methods subject the rock to a different stress and strain regime. Winkler, 1985, summarizes dispersion mechanisms. He points out the Biot mechanism, based on the solid frame “dragging” the pore fluid along with it. At low frequencies, expressions derived by the Biot theory and by Gassmann, 1951, allow the elastic properties of the fluid satu-

rated frame to be calculated from the properties of the dry frame and the fluid. The 'local flow' mechanism has been also discussed by many investigators, founded upon the inherent compliance of pore space. As an acoustic wave deforms the pore space, pore fluid will tend to flow from the compliant regions to the less compliant areas. It can be seen that the frequency and the level of saturation may impact acoustic response.

- **Pore and Microcrack Structure:** It can be observed, even from the earliest references, that pore and microcrack configurations impact the values of the static and to some extent the dynamic measurements. Many researchers have attributed the dynamic modulus being greater than the static modulus to the interlocking of sliding crack surfaces. This in turn related the discrepancies between the dynamic and static moduli to the stress levels applied during the measurements. Appropriate references include Zisman, 1933, Ide, 1936, Wyllie, 1956, Simmons and Brace, 1965, Walsh, 1965, O'Connell and Budiansky, 1974, Anderson et al, 1974, Kuster and Toksoz, 1974, Bruner, 1976, Cheng and Toksoz, 1979, and Marko and Nur, 1978. Howarth, 1985, stated:

“The discrepancies between E_D and E_S have been widely attributed to microcracks and pores, though the situation is complicated by the fact that results are dependent upon both rock microstructure and level of confinement and both E_D and E_S are affected differently.”

- **Confining Pressure:** The foregoing section alludes to the influence of microcracks and pores on wave transmission. Consider the following:

- At low to no confining pressure, static loading will sense the bulk material characteristics, including the presence of open and sliding cracks which lead to a smaller stiffness. However, the acoustic waves, which transmit mainly through the matrix of a rock, are only marginally influenced by the cracks.

- With the application of confining pressure, dynamic moduli increase moderately, with crack closure. With application of confining pressure, static moduli increase substantially as the bulk medium deforms less (Zheng et al. 1991).

- **Saturation:** All of the aforementioned evidence suggests that moduli are sensitive to the pore structure, the accompanying effective stress and the fluid in the pores (i.e. bulk modulus of fluid).

Evidently, this is an extremely complicated problem with ramifications for field design, where dynamic logging measurements are routinely used to infer static or quasi-static material properties. The complexity of the situation often precludes generalization, and individual lithologies should be treated distinctly. This is particularly appropriate for

coal which exhibits characteristics distinct from many more conventional lithologic members. The limited coal literature has been summarized by Yu et al (1990, 1991). Much of the published work concentrates on measurements of dynamic mechanical properties of coal, with limited comparison to statically determined properties. An exception is Zipf and Bieniawski, 1990. The primary intent of this document is to provide some comparisons of static and dynamic response of coal, with hypotheses rationalizing behavior as appropriate.

UNIQUE CHARACTERISTICS OF COAL

Coal is a cleated, and often friable material, containing two different types of pore space. These are the "matrix" micropore porosity and the "cleat" porosity. The matrix permeability is often assumed to be in the ηd range and the bulk permeability for coal is for most practical purposes assumed to be the cleat permeability. Cleat system closure makes the bulk permeability highly stress dependent. These characteristics set coal apart from many other geologic materials. Mechanical tests on a medium volatile bituminous coal from Pennsylvania have indicated that in general the behavior of this coal under quasi-static loading may be characterized as follows:

- a. The mechanical properties (e.g., moduli) are isotropic under isotropic (hydrostatic) loading,
- b. The mechanical properties are isotropic under anisotropic loading (e.g., triaxial loading) mainly in the absence of pore/cleat pressure,
- c. The mechanical properties are anisotropic for all other loading conditions.

The above observations indicate that the presence of cleat pressure significantly affects the response of coal to mechanical loading. Since there are probably limited chemical interactions between the typical pore fluid (i.e., water) and coal, it may be concluded that the described mechanical behavior is caused by the cleat-fluid interaction.

The interaction between cleats and pore fluid is evident in Figure 1, which shows the results of cyclic triaxial loading on a single coal specimen at 2000 psi (13.79 MPa) confining pressure. In this test, a cylindrical coal specimen, 2 inches in diameter by 4 inches long, was axially (i.e., normal to the bedding planes and parallel to the face and butt cleats) loaded and unloaded at 500, 1000, and 1500 psi (3.448, 6.897 and 10.345 MPa) pore/cleat pressures, respectively, in order to determine the effect of increasing pore pressure levels. This loading procedure resulted in axial elastic moduli of 470, 410, and 310 ksi (3241, 2828 and 2138 MPa), respectively, and Poisson's ratios of 0.28, 0.30, and 0.35, respectively. During the last loading cycle, performed at 1500 psi cleat pressure, the specimen failed at an axial stress difference of approximately 1850 psi. Although the reduction in the elastic modulus and strength as well as the increase in Poisson's ratio, are also expected for granular rocks under the same conditions, these responses are magnified in coal due to its

cleated nature. It may be speculated that with the axial stress being greater than the confining stress, fluid flow occurs from the features perpendicular to the maximum stress into the cleats parallel to the maximum stress (in this case the axial stress). The important observation is the significance of the cleat pressure on static mechanical properties.

Figure 2 represents failure surfaces constructed using the compiled data from a number of mechanical tests performed at zero and at elevated pore pressures. In this figure, the deviatoric shear stress ($\sqrt{J_2'}$) at failure has been plotted versus the effective hydrostatic stress ($J_1'/3$). The prime (') denotes the effective stress as given by $\sigma' = \sigma - \alpha P_p$, with Biot's coefficient (α) assumed to be equal to 1 (i.e., equivalent to Terzaghi's effective stress concept). Note that by using this equation for calculation of the effective stresses, it has been inherently assumed that Biot's effective stress concept is applicable to tight, cleated media.

The solid line in Figure 2 represents the failure surface for a range of triaxial tests performed at zero pore/cleat pressure (solid squares) under quasi-static loading; the dashed line represents the data for tests at elevated, constant pore/cleat pressure. The difference between the two failure surfaces could have been caused by one or a combination of (1) heterogeneous nature of coal (the cleat system), and (2) loading path dependence. In the absence of pore pressure, isotropic moduli have been evidenced for coal under all stress regimes. However, presence of pore pressure appears to result in anisotropic material properties under non-hydrostatic loading. The features perpendicular to the direction of the maximum "total" stress may not be opened and/or saturated to the same degree as the features in other directions. Some reduction in the coal strength may also be attributed to the fact that the fluid trapped within the cleats (i.e., triaxial tests represented by solid circles in Figure 2) tends to have a "lubricating" effect which is enhanced by the low permeability of the coal matrix. Regardless of the reasons behind the differences between the two failure surfaces, the data presented to this point clearly demonstrates the uniqueness of coal as compared with other geologic materials and the dependence of its mechanical properties on the fluid-cleat interaction. Fluid-cleat interaction should be expected in measurement of the dynamic properties of coal.

SPECIMEN PREPARATION

Obtaining coal properties in the laboratory is problematic due to the difficulties associated with recovery of intact specimens for testing. Specimen preparation techniques used for intact rocks are inadequate for most types of coal, due to their friable nature. For example, coring a small cylindrical specimen of coal usually results in disintegration and breakage. Furthermore, for those specimens which "appear" to be intact, the degree of disturbance and its effect on material properties is unknown.

In a recent study related to hydraulic fracturing of coal (Khodaverdian et al. 1991a, 1991b), several techniques were examined by the authors for obtaining intact core specimens for mechanical testing from a highly friable, medium volatile coal. These

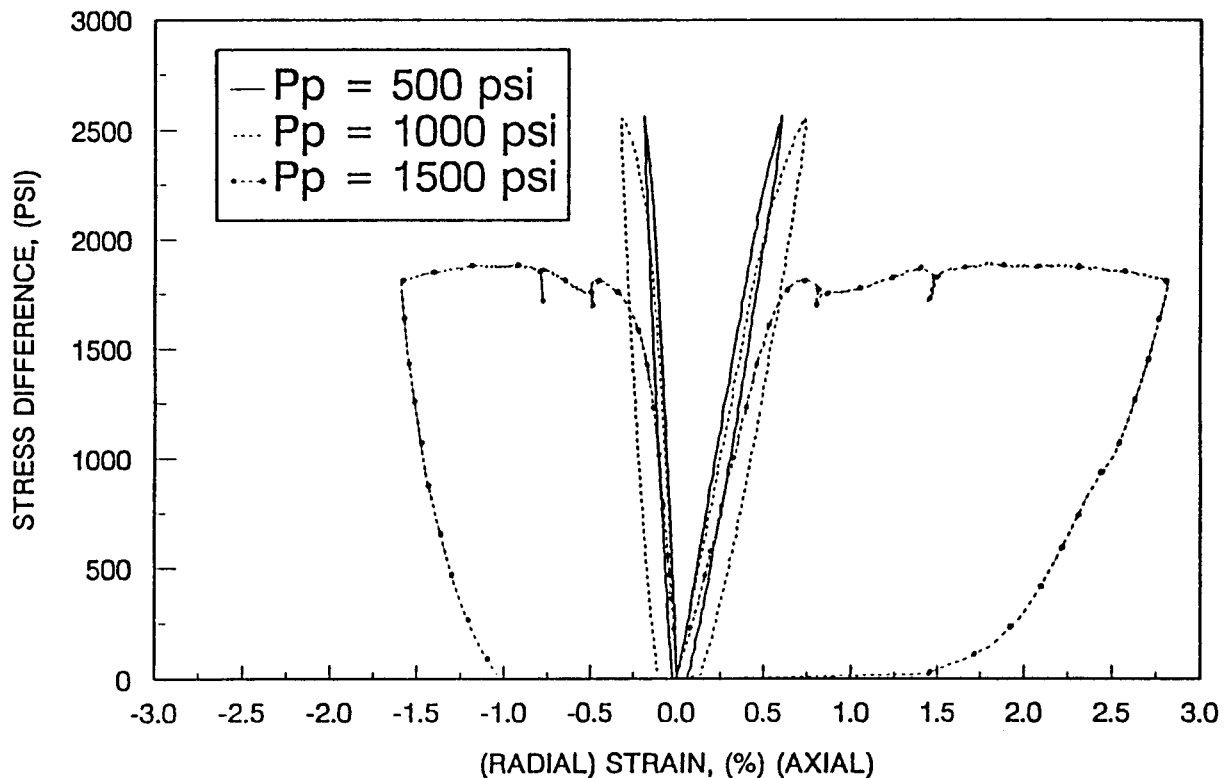


Figure 1. Cyclic triaxial testing results for a single coal specimen at a confining pressure of 2000 psi.

techniques included coring of the specimens using, stepwise grinding (instead of coring) the test specimen into a polygon of the desired diameter, and water-saturated freezing and subsequent coring to avoid disintegration of the coal. Another technique, which has not yet been tried, is dry-freezing of coal (at temperatures below -30° F and low moisture content) prior to and during coring of the specimen. This would be preferable to water-saturated freezing since it is expected to reduce cleat disturbance caused by fluid expansion during freezing.

Of all the techniques tried to date, stepwise grinding has proven to cause the least disturbance to the cleats. This technique was adopted for specimen preparation. First, a prismatic block of medium volatile bituminous coal with its axis parallel to the face and butt cleats, was saw-cut from a larger coal block. Subsequently, the sides of the specimen were ground in a stepwise fashion until the cross-section of the prism was formed into a 60-sided equilateral polygon, approximately 2 inches in diameter. Finally, the specimen (prism) was cut to length and its ends were ground to obtain flat and parallel surfaces within ± 0.001 ", for loading with endcaps.

The coal used in this research was surface mined and hence was assumed to be degassed. After machining, the specimens were dried in an oven at a constant temperature

of 105°C for 72 hours. A vacuum of 25 psi was applied to the specimens after oven drying to minimize initial moisture content.

EXPERIMENTAL PROCEDURES

Before testing, the coal specimens were placed between two stainless steel endcaps and jacketed with a Teflon sleeve to prevent intrusion of the confining fluid and to separate the confining pressure from the pore pressure. The stainless steel endcaps contained transducers so that ultrasonic wave velocity measurements could be performed concurrently with static mechanical property measurements. Strain-gaged cantilevers for axial and radial strain measurement were then mounted on the jacketed specimen. The strain measurement instrumentation is accurate to 0.001% strain. The fully instrumented specimen was then placed inside a pressure vessel capable of applying pressures of up to 50,000 psi.

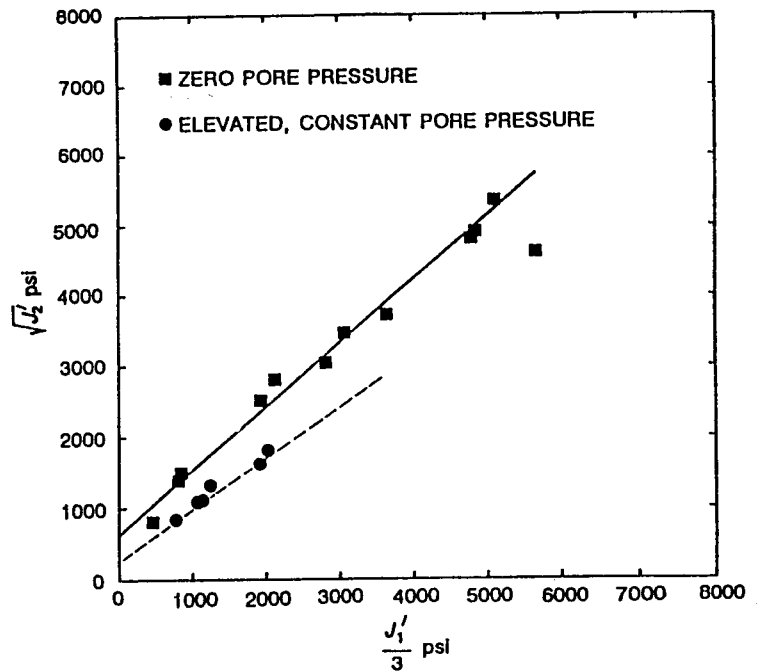


Figure 2. Failure surfaces for drained and undrained tests.

Stress path experiments were performed on the dry specimens after vacuuming. A hydrostatic confining pressure was applied in steps of 500 psi at a rate of 2 psi/sec, while the axial and radial strain were monitored continuously. At the end of each loading step, ultrasonic (1 MHz frequency) compressional (P) and shear (S) waves were transmitted through the sample length. From the received wave forms, the times for P and S waves to travel through the specimen were measured and their velocities calculated. The velocities were later used for determination of dynamic mechanical properties. After the confining pressure reached a designated level (3000 psi in this case), an axial differential stress was applied in steps of 500 psi, under axial strain control (10^{-5} in/in/sec), while the confining pressure was maintained constant. At the end of each step, ultrasonic wave velocities were measured; the static properties were determined using the conventional stress-strain data.

In order to measure the effect of saturation on both static and dynamic properties of coal, multitherm, a low viscosity oil, was used for saturation. Before saturation, apparent porosity was determined using Helium gas. An initially dry specimen which was Teflon jacketed and instrumented with strain-gaged cantilevers, was placed in the pressure vessel. To saturate the specimen, a vacuum pressure of 25 psi was applied to testing system for 1 hour. The system was then back-flooded with multitherm oil. From the amount of multitherm injected into the specimen, the degree of saturation was inferred. A hydrostatic

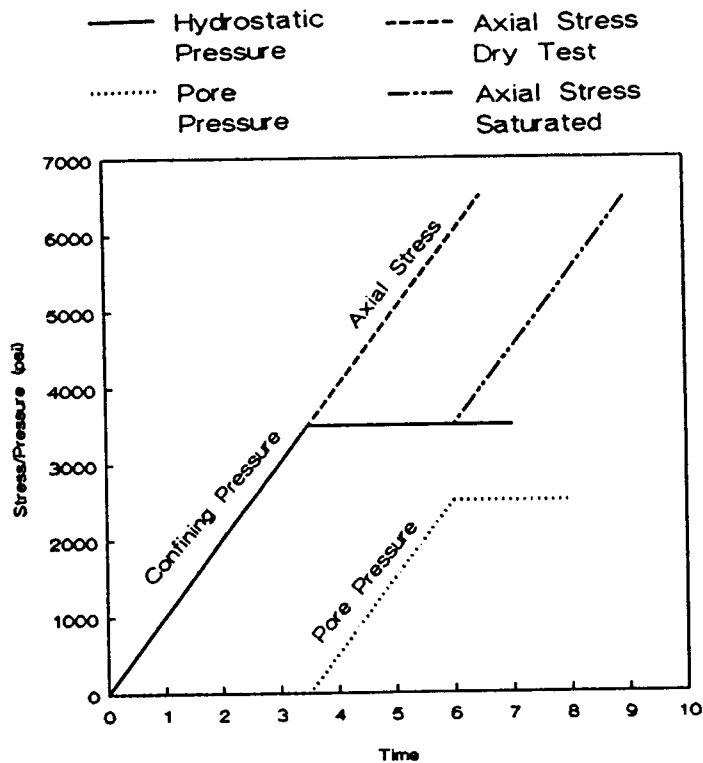


Figure 3. Stress path for concurrent static-dynamic property determination.

of samples were 2 inches in diameter by 4 inches long, with an apparent porosity of 4.2%. These samples were tested under cleat system saturation levels of 0%, 41.9%, and $\approx 100\%$. Samples from a different mine in the same field, with an apparent porosity of 7.1%, were tested at inferred cleat system saturation levels of 0% and $\approx 100\%$. In the following discussion, the low porosity coal is referred to as Coal No. 1, and the high porosity coal is referred to as Coal No. 2.

Figure 4 and 5 are plots of the dynamic moduli and Poisson's ratio versus the static modulus and Poisson's ratio for all samples tested under all stress conditions. As has been indicated by many researchers in literature on other rocks, coal also exhibited higher dynamic than static moduli, Figure 4. Some data points fell below the 45° line at low stress conditions. Poisson's ratio for the coal samples also showed similar behavior to other rocks, i.e., no obvious static-dynamic relationship. As can be seen in Figure 5, the dynamic Poisson's ratio can be either greater or less than the static Poisson's ratio. Coal No. 1 did show an increase in dynamic Poisson's ratio as the saturation level changed from 0% to $\approx 100\%$. This increase resulted from a reduction in shear-wave velocity in the saturated samples and will be discussed subsequently. Due to the limited number of samples and saturation levels tested, conclusions on Poisson's ratio as a function of saturation level cannot be readily made.

Figure 6 is a plot of the static and dynamic bulk moduli as a function of increasing hydrostatic confining pressure (refer also to Figure 3), when pore pressure was zero, at different saturation levels. The open symbols represent static results and the solid symbols

confining pressure was applied in steps of 500 psi as the pore pressure was maintained at atmospheric pressure, and ultrasonic velocities were measured at the end of each step until the confining pressure reached 3500 psi. Pore pressure was then increased from 0 to 2500 psi. After equilibration an axial differential stress was applied. Figure 3 shows the stress paths described. During both hydrostatic and axial loading, ultrasonic velocities were measured periodically.

RESULT AND DISCUSSION

Two types of coal were used for concurrent static and dynamic property measurements. One set

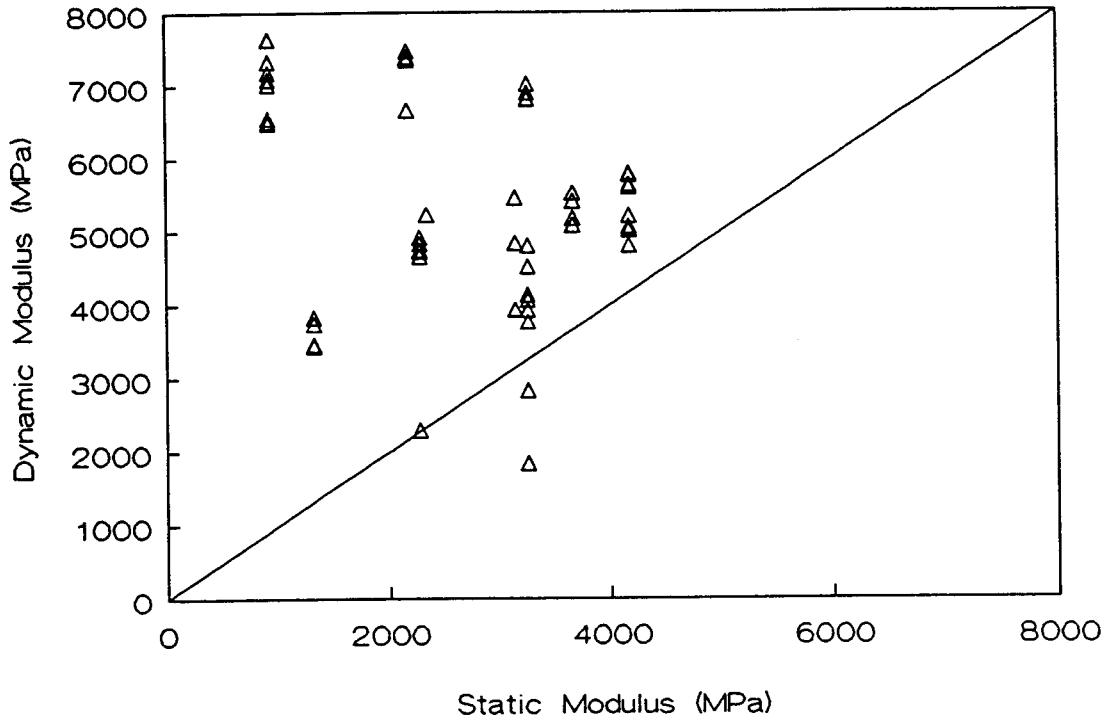


Figure 4. Static Young's and bulk moduli versus dynamic Young's and bulk moduli.

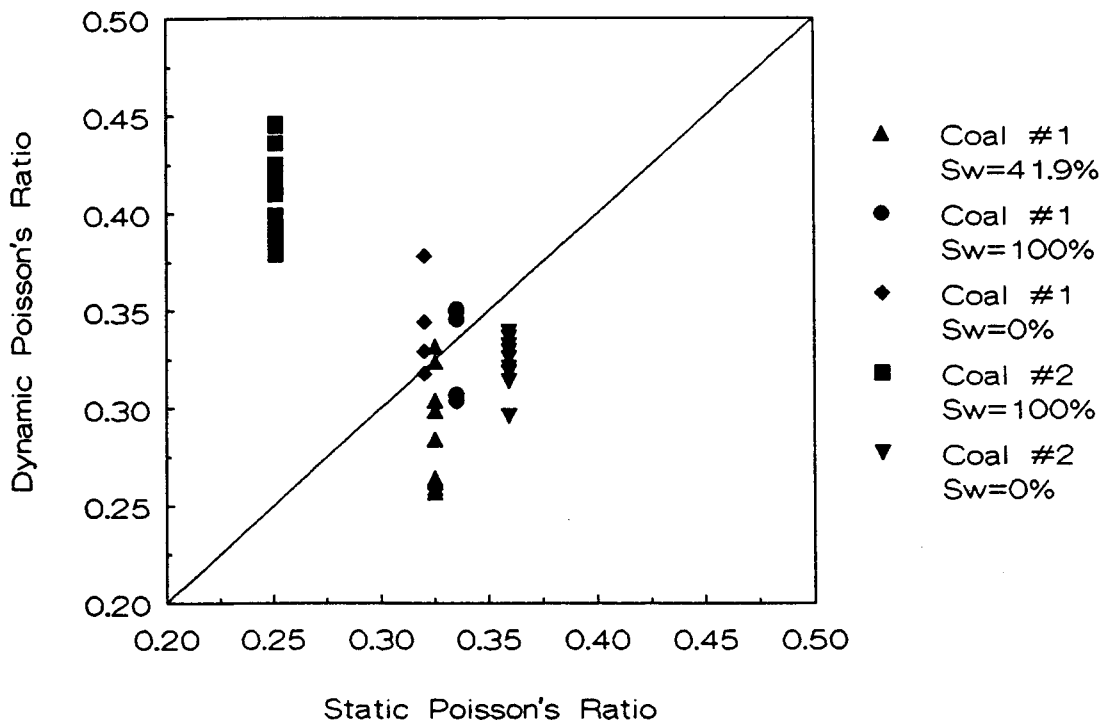


Figure 5. Static Poisson's ratio versus the dynamic Poisson's ratio.

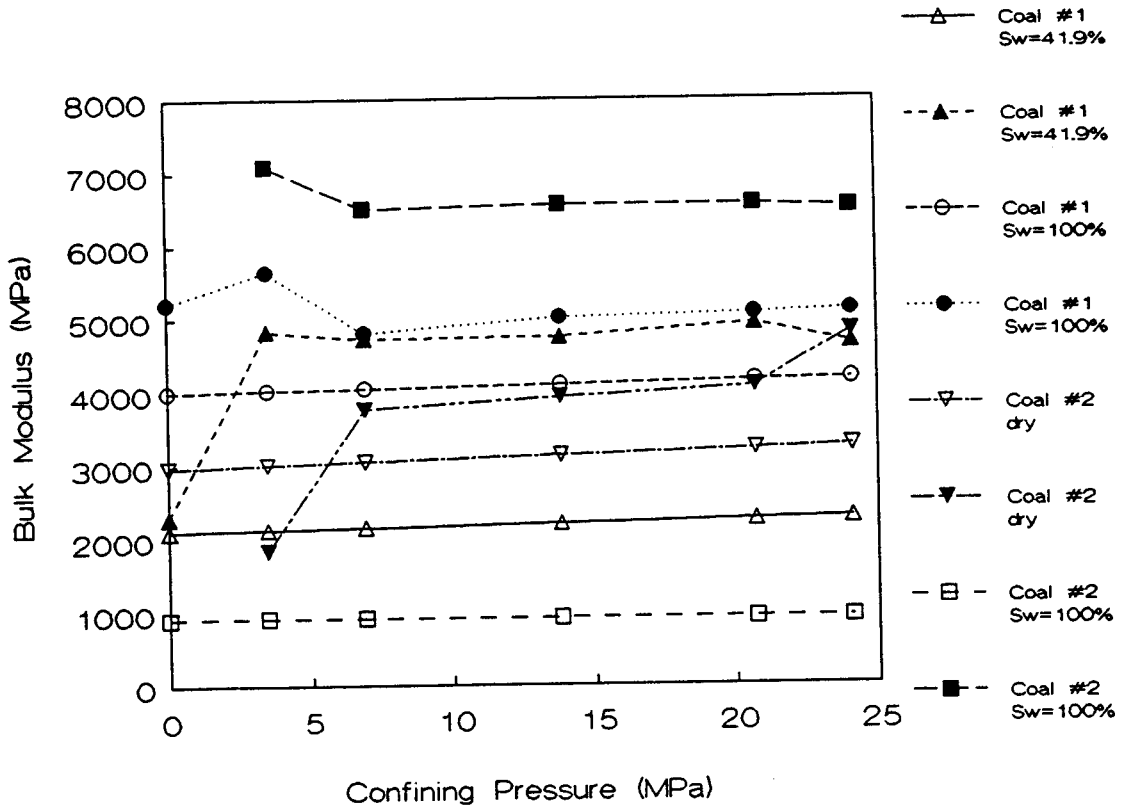


Figure 6. Static and dynamic moduli as functions of hydrostatic confining stress.

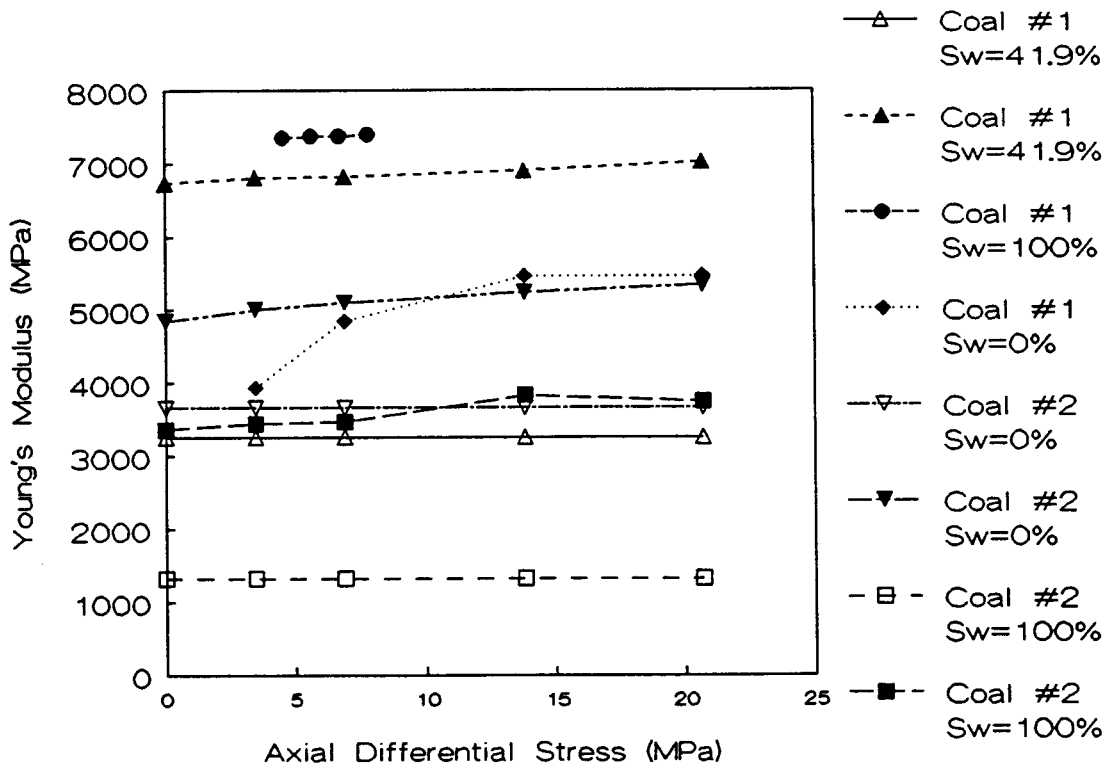


Figure 7. Static and dynamic Young's moduli during triaxial compression.

represent the dynamic results. At the lowest hydrostatic confining stress levels, the dynamic bulk modulus varies more rapidly than the static bulk modulus does. After the confining stress reached 1000 psi (6.9 MPa), both static and dynamic moduli increased very slightly. One difference between the dynamic behavior of the fully saturated and the partially saturated samples is that the fully saturated samples have a high dynamic modulus at low stress levels, remaining relatively unchanged as the confining stress increased. On the other hand, the dry and partially saturated samples have low dynamic modulus at low confining stress levels and the modulus increased with increasing confining stress.

Figure 7 shows Young's Modulus (static and dynamic) as a function of axial differential stress during triaxial compression (confining stress of 3500 psi as shown in Figure 3). The dynamic moduli showed less variation as the axial differential stress was increased than did the dynamic bulk moduli during initial portions of the hydrostatic compression, with the exception of the dry sample from Coal No. 1. The smaller modulus variation during triaxial compression than during hydrostatic compression may be due to closure of fractures and redistribution of the pore fluid during hydrostatic compression. A coal sample, in a relaxed state, before being subjected to any stress, has many open, low stiffness fractures/cleats. During initial hydrostatic compression, these low stiffness features tend to close. This is evident from static stress-strain curves. This behavior is not seen in Figure 6 because it took place at confining stress below 50 psi. During initial hydrostatic compression, the dynamic properties are more sensitive to the presence of fractures/cleats and other discontinuities and can vary by great amounts. During subsequent hydrostatic and triaxial compression, the discontinuities with low stiffness have already been closed or compacted, and the overall deformation of samples comes from small elastic deformations of the matrix and the fractures.

The effect of the saturation level on the dynamic properties of coal is not immediately obvious. Both Figures 6 and 7 show that the dynamic moduli for Coal No. 1, increased with an increase in saturation level. However, dynamic moduli for Coal No. 2, with a higher apparent porosity, decreased with an increase in saturation level. Examination of P- and S-wave velocities suggests a cause for such different behavior. Figures 8 and 9 show the variations of P- and S-wave velocities as functions of effective mean stress. Figure 8 indicates that as the saturation level increases, the P-wave velocity increases. It is hypothesized that liquid in the discontinuities increases compressive wave transmissivity due to its higher stiffness (lower compressibility) as compared to air or vacuum. Figure 9, however, indicates a decrease in S-wave velocity as the saturation level is increased. However, the literature shows that the S-wave velocity is often found to increase with elevated saturation in other rocks. This may result from the dominant presence of cleats. In many porous rocks, the pores have an aspect ratio (ratio between the longest axis and the shortest axis of a pore) which may be close to unity; the transmission of S-waves may occur indirectly through compression of the fluid against the matrix material on the pore walls (mode conversion). In coal, where the majority of pore space consists of features which are orthogonal and parallel to the direction of S-wave vibrations, the pore fluid in the features parallel to the vibration is hypothesized to function as a wave damping layer. When no pore fluid is present, the transmission of S-waves is

through the contact of matrix material and “interlocking” of asperities in fractures/cleats.

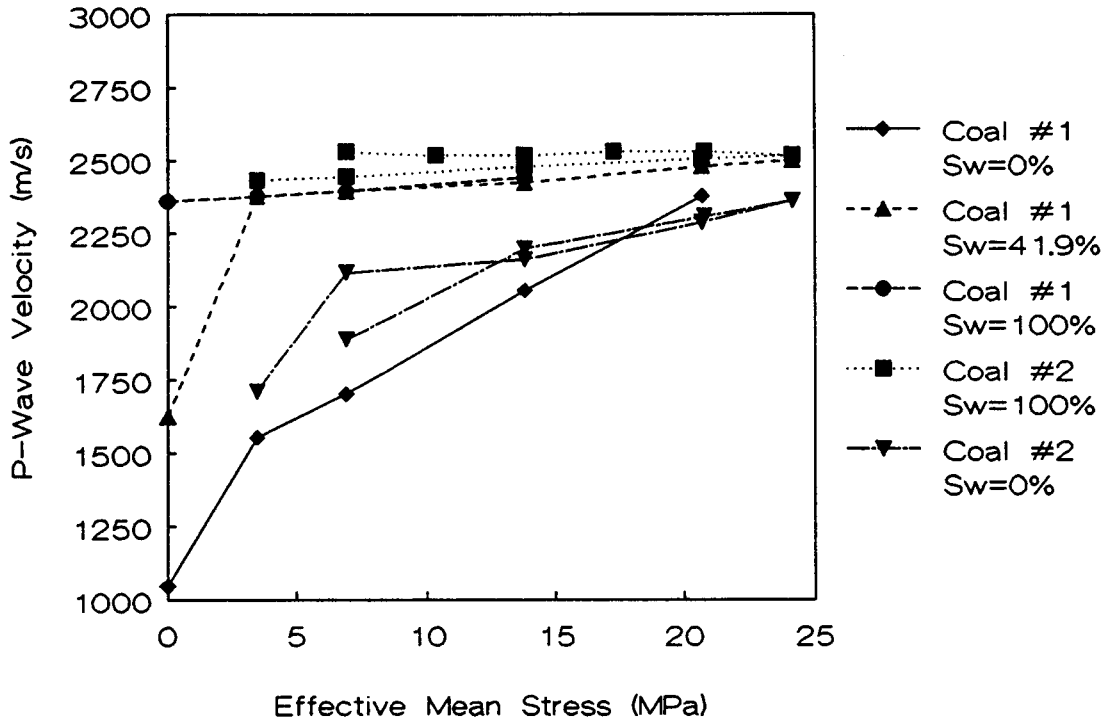


Figure 8. P-wave velocity as a function of effective stress.

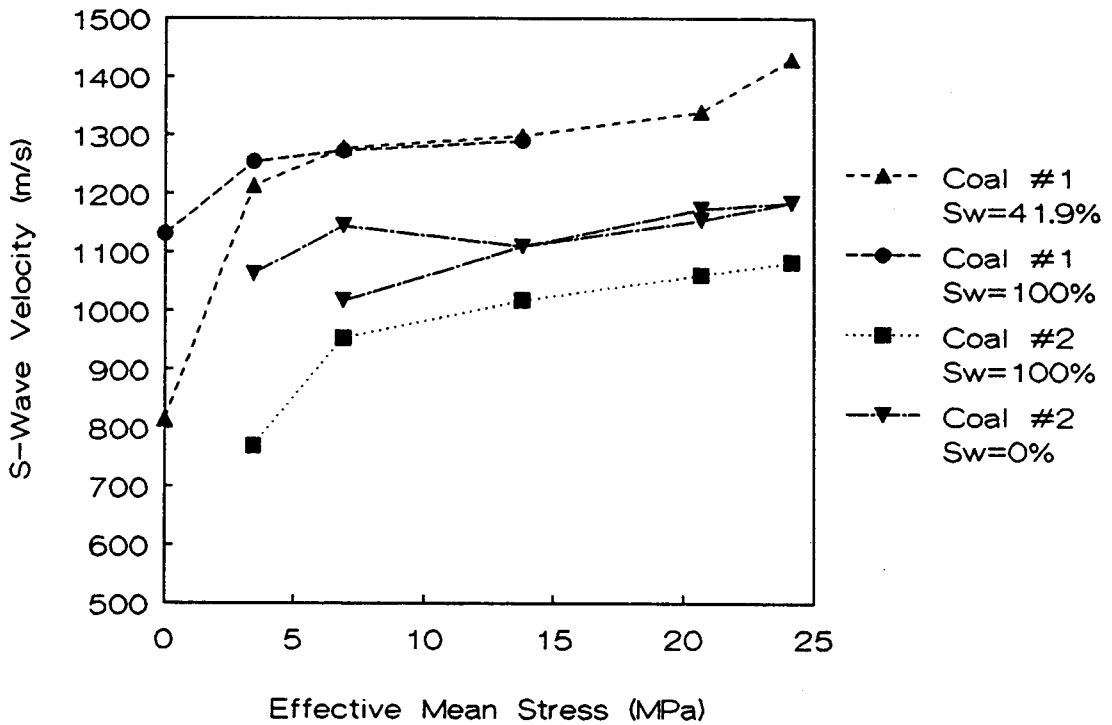


Figure 9. S-wave velocity as a function of effective stress.

When pore fluid is present in a cleat/fracture, the fluid tends to drive the fracture surfaces apart so that less contact area exists between the surfaces. The transmission of S-waves across the fracture is through the viscous force generated by shearing in the pore fluid. This transmitted force, even in an ultra thin layer, is much less than the force generated by compression of the fluid. With higher cleat/fracture density, especially those orthogonal to the propagation direction of shear waves, more reduction in the S-wave velocity is expected when pore fluid exists. Coal samples with higher porosity (7.1%) exhibited such behavior.

It is necessary to state that material variability also plays an important factor in coal static and dynamic properties. In order to examine the material variability effect, many samples with similar proximate analyses and maceral content need to be evaluated.

CONCLUSIONS

The following conclusions can be drawn from the concurrent static and dynamic property measurements and observations:

1. The dynamic moduli (Young's and bulk) are greater than the static moduli. This is consistent with the behavior of other rocks.
2. The dynamic properties of coal are more sensitive to stress variations when the effective stress level is low.
3. P-wave velocity increases as the level of saturation increases. For the tested, this behavior is the same as for other rocks types. S-wave velocities decreased as the level of saturation increased. It is hypothesized that this is due to the cleat/fracture system in the coal, arguing that the pore fluid damped S-wave propagation by reducing the solid-solid contact area. With higher cleat porosity, more reduction in S-wave velocity might be expected, when pore fluid is present. At constant confining stress, an increase in pore pressure also reduces the S-wave velocity because higher pore pressure can induce more separation of fracture surfaces and less contact area.
4. Based on elastic equations from which dynamic Young's modulus and Poisson's ratio were derived, an increase in V_p and a decrease in V_s with increasing saturation as seen from the tests, yielded an increased value for Poisson's ratio and either an increased or decreased value for elastic modulus, depending on the degree of change in P and S wave velocities.
5. Limited evidence suggests that the most significant reduction in shear wave velocity may take place at relatively low saturation levels. When saturation reaches a certain level, reduction in the S-wave velocity levels out. On the low porosity coal tested, this saturation level is speculated to be less than 42%.

6. Due to the limited number of samples tested, many other factors that definitely influence dynamic properties of coal have not been explored. These factors include coal anisotropy, relative orientation of the S-wave vibrations to the cleat system orientation, presence of different fluids, temperature, additional saturation levels and other material variabilities.

REFERENCES

- Anderson, D. L., Minster, B. and D. Cole, "The Effect of Oriented Cracks on Seismic Velocities," *J.G.R.*, Vol. 79, No. 26, Sept. 1974.
- Bruner, W. M., "Comments on Seismic Velocities in Dry and Saturated Cracked Solids", by Richard J. O'Connell and Bernard Budiansky," *J.G.R.*, Vol. 81, No. 14, May 1976.
- Cannaday, F. X., "Modulus of Elasticity of a Rock Determined by Four Different Methods," Washington, U.S. Dept. of the Interior, Bureau of Mines, 1964.
- Cheng, C. H. and M. N. Toksoz, "Inversion of Seismic Velocities for the Pore Aspect Ratio Spectrum of a Rock," *J.G.R.*, 84, pp. 7533-7543, 1979.
- Gassmann, F., "Elastic Waves Through a Packing of Spheres," *Geophysics*, 16, pp 673-685, 1951.
- Howarth, D. F., "Development and Evaluation of Ultrasonic Piezoelectric Transducers for the Determination of Dynamic Young's Modulus of Triaxially Loaded Rock Cores," *Geotechnical Testing Journal*, GTJODJ, Vol. 8, No. 2, pp. 59-65, June 1985.
- Ide, J. M., "Comparison of Statically and Dynamically Determined Young's Modulus of Rocks," *Proc. Nat'l. Acad. Sci.*, Vol. 22, No. 2, Feb. 1936.
- Jeffrey, R. G. and J. D. McLennan, "Dynamic Versus Static Elastic Constants of Rock Samples from Well SFE-2", Reports to GRI, March 1989.
- King, M. S., "Ultrasonic Compressional and Shear Wave Velocities of Confined Rock Samples," *Proc. Fifth Can. Rock Mech. Symp.*, CIMM, Toronto, 1968.
- King, M. S., "Elastic Wave Velocities in Quartz Monzonite at Different Levels of Water Saturation," *Int. J. Rock Mech. Min. Sci. & Geomech. Abstr.*, Vol. 21, No. 1, pp. 35-38, 1984.
- Khodaverdian, M., McLennan, J. D. and A. H. Jones, "Spalling and the Development of a Hydraulic Fracturing Strategy for Coal," *Final Report Submitted to the Gas Research Institute (GRI)*, Contract No. 5087-214-1460, Terra Tek Report, TR91-111, April 1991.

- Khodaverdian, M., McLennan, J. D., Jones, A. H. and R. A. Schraufnagel, "Influence of Near Wellbore Effects on Treatment Pressure in Coal," *Proceedings of the 1991 Coalbed Methane Symposium*, Tuscaloosa, Alabama, May 1991.
- Kuster, G. T. and M. N. Toksoz, "Velocity and Attenuation of Seismic Waves in Two-Phase Media. Part I - Theoretical Formations," *Geophysics*, 39, pp. 587-606, 1974.
- Lin, W., "Ultrasonic Velocities and Dynamic Elastic Moduli of Mesa Verde Rocks," Unconventional Gas Program, Western Gas Sands Research, UCID-20273- Rev. 1, Mar. 1985.
- Marko, G. and A. Nur, "The Effect of Non-Elliptical Cracks on the Compressibility of Rocks," *J.G.R.*, 83, pp. 4459-4468, 1978.
- O'Connell, R. J. and B. Budiansky, "Seismic Velocities in Dry and Saturated Cracked Solids," *J.G.R.*, 84, pp. 3532-3536, 1979.
- Simmons, G. and W. F. Brace, "Comparison of Static and Dynamic Measurements of Compressibility of Rocks," *J.G.R.*, Vol. 70, No. 22, pp 5649-5656, Nov. 1965.
- Winkler, K. W., "Dispersion Analysis of Velocity and Attenuation in Berea Sandstone," *J.G.R.*, Vol. 90, No. 138, pp 6793-6800, Jul. 1985.
- Wyllie, M. R. J., Gregory, A. R. and L. W. Gardner, "Elastic Wave Velocities in Heterogeneous and Porous Media," *Geophysics*, Vol. XXI, No. 1, pp 41-70, Jan. 1956.
- Yu, G., Vozoff, K. and D. W. Durney, "P-wave Velocity in a Sydney Basin Coal: Dependence on Confining Pressure and Water Saturation," *Advances in the Study of the Sydney Basin, Proceedings of the 24th Symposium*, Newcastle, N.S.W. Australia, pp 130-137, 1990.
- Yu, G., Vozoff, K. and D. W. Durney, "Effect of Pore Pressure on Compressional Wave Velocity in Coals," *Exploration Geophysics*, 22. No.2, pp 475-480, 1991.
- Zheng, Z., McLennan, J. D. and J. W. Martin, "Compressive Stress-Induced Microcracks and Effective Elastic Properties of Limestone and Concrete", *Phase I Final Technical Report to U.S.A.F.*, Topic No. AF90-186, Terra Tek Report TR91-107, 1991.
- Zisman, W. A., "Young's Modulus and Poisson's Ratio with Reference to Geophysical Applications," *Proc. Nat'l Acad. Sci.*, 19,653, 1933.
- Zipf, R.K. and Z. T. Bieniawski, "Mixed-Mode Fracture Toughness Testing of Coal," *Int. J. of Rock Mech. Min. Sci. & Geomech. Abstr.*, V. 27, No.6, pp 479-493, 1990.

